

A NEW ROBOTIC HAND BASED ON THE DESIGN OF FINGERS WITH SPATIAL MOTIONS

Pol Hamon

Armor Méca
ZI La Grignardais
22490 Pleslin-Trigavou, France
Email: Pol.Hamon@armor-meca.com

École Centrale de Nantes/LS2N
UMR CNRS 6004, 1 rue de la Noe
44321 Nantes, France

Damien Chablat, Franck Plestan

Ecole Centrale de Nantes, LS2N
UMR CNRS 6004, 1 rue de la Noe, 44321 Nantes, France
Email: Damien.chablat@cnrs.fr, Franck.Plestan@ec-nantes.fr

ABSTRACT

This article presents a new hand architecture with three under-actuated fingers. Each finger performs spatial movements to achieve more complex and varied grasping than the existing planar-movement fingers. The purpose of this hand is to grasp complex-shaped workpieces as they leave the machining centres. Among the taxonomy of grips, cylindrical and spherical grips are often used to grasp heavy objects. A combination of these two modes makes it possible to capture most of the workpieces machined with 5-axis machines. However, the change in grasping mode requires the fingers to reconfigure themselves to perform spatial movements. This solution requires the addition of two or three actuators to change the position of the fingers and requires sensors to recognize the shape of the workpiece and determine the type of grasp to be used. This article proposes to extend the notion of under-actuated fingers to spatial movements. After a presentation of the kinematics of the fingers, the problem of stability is discussed as well as the transmission of forces in this mechanism. The complete approach for calculating the stability conditions is presented from the study of Jacobian force transmission matrices. CAD representations of the hand and its behavior in spherical and cylindrical grips are presented.

1 Introduction

Robotic hands are inspired by human ones to enable robots to grasp parts or tools. They can be used for industrial robots, for humanoid robots or as prostheses for humans. Since the early 1980s, many hands have been designed as the Okada hand [1], the Stanford/JPL hand [2], the Utah/MIT hand [3], the LMS hand [4]. This first generation of hands suffered many disadvantages such as their cost and the complexity of their control. Other hands have been developed by reducing the number of actuators and the number of degrees of freedom [5] [6]. Another way is the creation of under-actuated hands allowing the number of actuators to be reduced without reducing the number of degrees of freedom [7].

The architecture of these under-actuated fingers has not changed since their origin and remains planar. In order to adapt to the objects to be grasped, a mechanism placed at the base of each finger must be used to switch from a cylindrical to a spherical or planar grasp [7]. In this case, one or two actuators are required to change the type of grasp.

However, among the taxonomy of grips, the cylindrical and spherical grips are mainly used for gripping heavy objects [8]. The other types are for precision tasks and are not dedicated to the capture of heavy objects (Figure 1). To simplify both design and control, the aim of this article is to introduce a new finger architecture that can naturally adapt to the shapes of objects.

Next section presents the architecture of the new fingers.

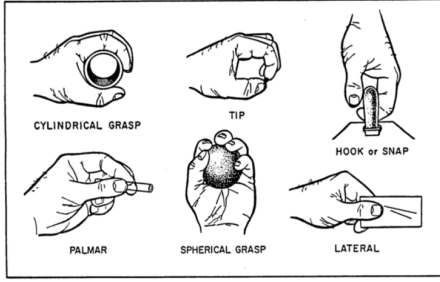


FIGURE 1: Grasping of common objects of the daily life

The equations of the kinematics are presented after the description of the different closed chains.

2 Architecture of the new hand

The purpose of this article is to present a new hand architecture, consisting of three fingers with a new architecture, the objective being to introduce a new type of spatial under-actuation.

2.1 Architecture of the new fingers

To achieve spherical and cylindrical grasps, an under-actuated finger architecture is presented featuring a spherical mechanism for the proximal phalanx [9] and four-bar mechanisms for the distal phalanges (Figure 2). This solution provides a new degree of freedom from under-actuated fingers allowing a non-planar behaviour comparable to the abduction movements of the human hand and thus a change in the type of grip. The hand is an under-actuated three-fingers assembly whose placement is defined to achieve both types of grasp.

The innovation of this architecture comes mainly from the use of the spherical mechanism. In order to simplify the geometry of the spherical parallel mechanism, we set $\|\vec{CO}_2\| = \|\vec{CO}_3\| = \|\vec{CO}_4\| = \|\vec{CO}_5\|$. In addition, the angles of the mechanism are two by two identical and defined as follows $\widehat{O_2CO_3} = \widehat{O_4CO_5} = \alpha$ and $\widehat{O_3CO_4} = \widehat{O_5CO_2} = \eta$.

A new actuating system is adapted to this new kinematics in order to meet the stability requirements when grasping objects. The four degrees of freedom of each finger can be defined as:

- A first degree of freedom θ_1 is defined as the movement of the proximal phalanx. θ_1 is the angle between $\vec{P_2C}$ and $\vec{P_2P_{11}}$
- A second degree of freedom θ_2 is defined as the movement of the spherical system. θ_2 is the angle between planes (C, O_2, O_3) and (C, O_2, O_5)
- A third degree of freedom θ_6 is defined as the movement of the intermediate phalanx. θ_6 is the angle between $\vec{O_5C}$ and $\vec{O_6O_7}$

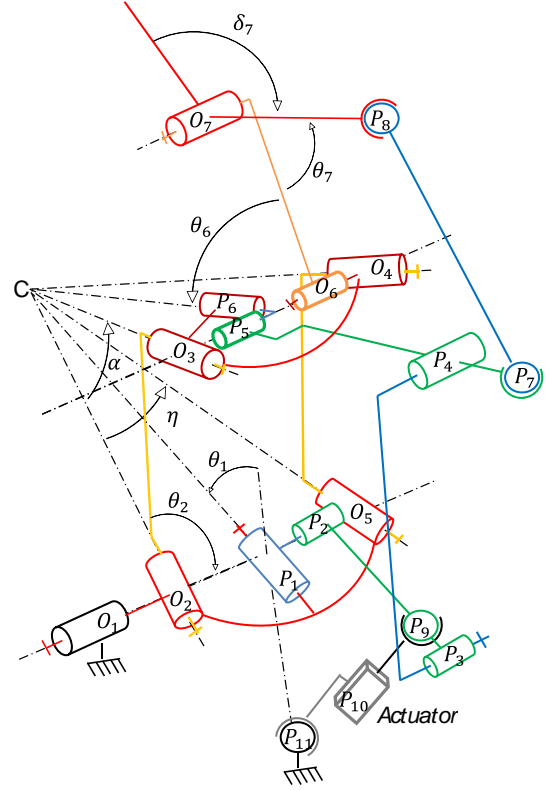


FIGURE 2: Kinematics of the new finger architecture

- A fourth degree of freedom θ_7 is defined as the movement of the distal phalanx. θ_7 is the angle between $\vec{O_7O_6}$ and $\vec{O_7P_8}$

By using spherical trigonometry [10] (Eq. (1)) and the results coming from the study of parallel spherical mechanisms [9] (Eq. (2)), the angles θ_1 , θ_2 , θ_6 and θ_7 read as:

$$\theta_1 = \frac{1}{2} \arccos \left(\frac{-\sin^2 \left(\frac{\eta}{2} \right) + \cos(\alpha)}{\cos^2 \left(\frac{\eta}{2} \right)} \right) \quad (1)$$

$$\theta_2 = -2 \operatorname{atan} \left(\sqrt{\frac{-\tan \left(\frac{\alpha}{2} \right) \tan \left(\frac{\eta}{2} \right) - 1}{\tan \left(\frac{\alpha}{2} \right) \tan \left(\frac{\eta}{2} \right) - 1}} \right) \quad (2)$$

$$\theta_6 = -\frac{1}{2} \arccos \left(\frac{2 \cos(\alpha) + \cos(\eta) - 1}{\cos(\eta) + 1} \right) - \pi/2 \quad (3)$$

$$\theta_7 = \pi - \delta_7 \quad (4)$$

The angles are defined as positive in the closing direction of the fingers.

2.2 Grasping and fingers' positions

Figure 3 shows, in a top view, the ideal positioning of the fingers to switch from prismatic to spherical grips. The lines

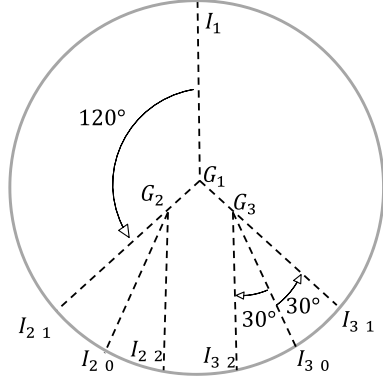


FIGURE 3: Fingers' positions for neutral, cylindrical, spherical grasps

$(I_1 G_1)$, $(I_{2-0} G_2)$, $(I_{3-0} G_3)$ represent the orientation of a normal vector on the surface of the distal joint when the three fingers are in the neutral position, the lines $(I_1 G_1)$, $(I_{2-1} G_1)$, $(I_{3-1} G_1)$ the orientation of a normal vector on the surface of the distal joint when the three fingers are in position to make a cylindrical grasp and the lines $(I_1 G_1)$, $(I_{2-2} G_2)$, $(I_{3-2} G_3)$ the orientation of a normal vector on the surface of the distal joint when the three fingers are in position to make a spherical grasp. Points G_1 , G_2 , G_3 correspond to the point C (Figure 2) of each finger.

Depending on the shape of the objects to be grasped, the posture of the fingers will be adjusted in a natural way. Springs will allow the fingers to return to a neutral posture in the absence of contact. Figure 4(a) depicts an example of the fingers positions for the spherical grasp and the Fig. 4(b) the cylindrical grasp.

3 Stability analysis

We generalize to this new finger architecture, the under-actuated finger stability theory used for planar fingers [11]. The stability criterion is defined as $\mathbf{f} \geq \mathbf{0}$ where f is the vector of the constraints of the finger phalanges on the gripping part. The values of \mathbf{f} is given by

$$\mathbf{f} = \mathbf{J}^{-t} \mathbf{T}^{-t} \mathbf{t} \quad (5)$$

where \mathbf{J} is the matrix of the torques on the degrees of freedom as a function of the forces applied on the phalanges, \mathbf{T} is the matrix of the torque ratios of the transmission mechanism and \mathbf{t} is the vector of the input force applied by the actuator.

Now the matrices \mathbf{T} and \mathbf{J} are calculated in order to obtain the expression \mathbf{f} . In the following sub-sections the methodology developed for planar under-actuated fingers [12] is followed to extend it to the new proposed spatial architecture.

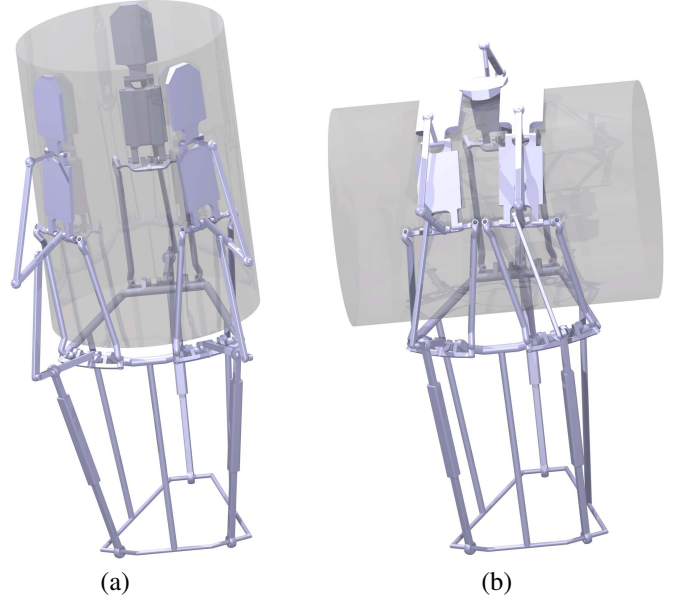


FIGURE 4: (a) Spherical grasp and (b) cylindrical grasp

3.1 Matrix of the torques \mathbf{J}

When picking up an object, contacts with the fingers can be located in four places, two at the spherical mechanism, one at the middle phalanx and one at the distal phalanx. Define the 4 forces f_1, f_2, f_3, f_4 (see Figure 5) which apply to the points S_1, S_2, S_3, S_4 . k_1, k_2, k_3, k_4 and q_3, q_4 are the distances between these points and the origin of the joints O_1, O_2, O_6, O_7 . m_1 and m_2 are the angles between the direction of the forces f_1, f_2 and the planes $(O_2 C O_3)$ and $(O_4 C O_5)$ so that the forces f_1, f_2 are parallel to the forces f_3, f_4 in the neutral position (home position).

By using spherical trigonometry [10], one gets

$$\begin{aligned} m_1 &= \frac{1}{2} \operatorname{acos} \left(\frac{\cos(\eta) - \sin^2 \left(\frac{\alpha}{2} \right)}{\cos^2 \left(\frac{\alpha}{2} \right)} \right) \\ m_2 &= -\frac{1}{2} \operatorname{acos} \left(\frac{\cos(\eta) - \sin^2 \left(\frac{\alpha}{2} \right)}{\cos^2 \left(\frac{\alpha}{2} \right)} \right) \end{aligned} \quad (6)$$

To carry out the computations, define a frame located in the middle of point O_2 and O_3 at point P_1 such that $\vec{R}_{1y} = \vec{P}_1 O_5$ and $\vec{R}_{1z} = \vec{P}_1 C$ and a frame located in C such that $\vec{R}_{2z} = \vec{O}_2 C$ and $\vec{R}_{2x} = \vec{R}_{1x}$. The matrix \mathbf{J} depends on the contact points of the

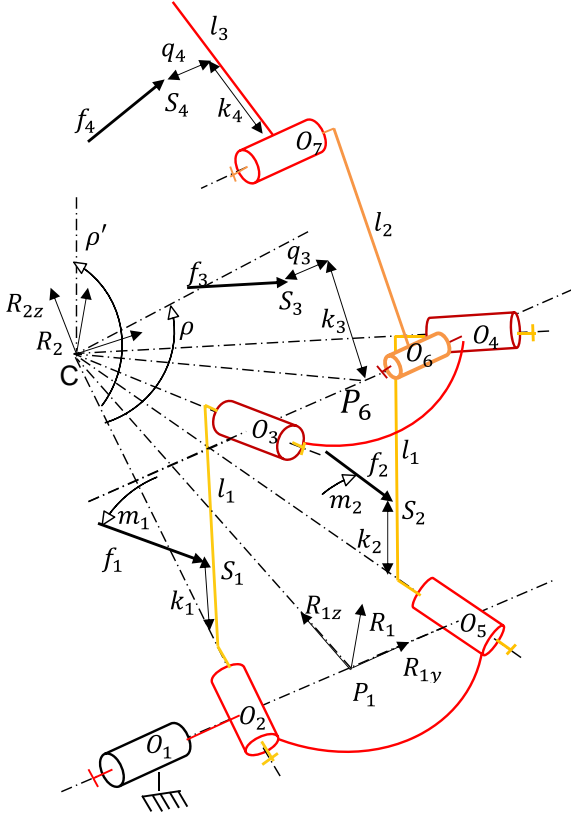


FIGURE 5: Matrix of the torques \mathbf{J}

finger

$$\mathbf{J} = \begin{bmatrix} \Theta_1 & \Theta_2 & 0 & 0 \\ \frac{\Theta_1}{f_1} & \frac{\Theta_2}{f_1} & 0 & 0 \\ \frac{\Theta_1}{f_2} & \frac{\Theta_2}{f_2} & \frac{\Theta_6}{f_4} & 0 \\ \frac{\Theta_1}{f_3} & \frac{\Theta_2}{f_3} & \frac{\Theta_6}{f_4} & \frac{\Theta_7}{f_4} \\ \frac{\Theta_1}{f_4} & \frac{\Theta_2}{f_4} & \frac{\Theta_6}{f_4} & \frac{\Theta_7}{f_4} \end{bmatrix} \quad (7)$$

where $\Theta_1, \Theta_2, \Theta_6, \Theta_7$ are the torques along the joint axes O_1, O_2, O_6, O_7 respectively. The ratios $\frac{\Theta_7}{f_4}, \frac{\Theta_6}{f_4}, \frac{\Theta_6}{f_3}$ are calculated in the same way as in the planar case [11]:

$$\frac{\Theta_7}{f_4} = k_4 \quad \frac{\Theta_6}{f_4} = k_4 - l_2 \cos(\delta_7 + \theta_7) \quad \frac{\Theta_6}{f_3} = k_3 \quad (8)$$

Furthermore, $\frac{\Theta_2}{f_2}$ and $\frac{\Theta_2}{f_1}$ can be calculated by using the formulae

of the spherical parallel mechanisms [9]

$$\begin{aligned} \frac{\Theta_2}{f_1} &= k_1 \sin(m_1) \cos\left(\frac{\alpha}{2}\right) \\ \frac{\Theta_2}{f_2} &= \frac{\Theta_2}{\Theta_5} k_2 \sin(m_2) \cos\left(\frac{\alpha}{2}\right) \\ \frac{\Theta_2}{\Theta_5} &= \frac{\sin(\rho)}{\sin(\rho - \eta)} \end{aligned} \quad (9)$$

with ρ the angle between the line (O_2C) and the intersection of planes (O_2CO_5) and (O_3CO_4) [9].

To evaluate $\frac{\Theta_2}{f_3}$ and $\frac{\Theta_2}{f_4}$, we calculate the ratio of the speed at the points of application of the forces to multiply them by their components in the R_2 reference frame.

$$\frac{\Theta_2}{\Theta_3} = \frac{\dot{\theta}_3}{\dot{\theta}_2} = \frac{\sin(\rho')}{\sin(\rho' - \alpha)} \quad (10)$$

where ρ' is the angle between the line (O_2C) and the intersection of the planes (O_2CO_3) and (O_4CO_5) [9]. Positions S_3, S_4 are calculated in the R_2 frame with

$$\begin{aligned} [S_{3x} \ S_{3y} \ S_{3z} \ 1]^t &= Rot_z(\theta_2) Rot_x(\alpha) \\ &Rot_z(\theta_3) Rot_x\left(\frac{\eta}{2}\right) Trans_z(-z_1) Rot_y(\theta_6) \\ &Trans_z(k_3) Trans_y(q_3) [0 \ 0 \ 0 \ 1]^t \end{aligned} \quad (11)$$

$$\begin{aligned} [S_{4x} \ S_{4y} \ S_{4z} \ 1]^t &= Rot_z(\theta_2) Rot_x(\alpha) \\ &Rot_z(\theta_3) Rot_x\left(\frac{\eta}{2}\right) Trans_z(-z_1) \\ &Rot_y(\theta_6) Trans_z(l_2) Rot_y(\theta_7) \\ &Trans_z(k_4) Trans_y(q_4) [0 \ 0 \ 0 \ 1]^t \end{aligned} \quad (12)$$

with, if $0 < \theta_2 < \pi$

$$\begin{aligned} \theta_3 &= -\text{atan}_2(B, A) + \text{acos}\left(\frac{C}{\sqrt{A^2 + B^2}}\right) \\ \text{else :} & \\ \theta_3 &= -\text{atan}_2(B, A) - \text{acos}\left(\frac{C}{\sqrt{A^2 + B^2}}\right) \end{aligned} \quad (13)$$

$$\begin{aligned} \text{with } A &= \sin^2(\alpha) \cos(\eta) \cos(\theta_2) - \sin(\alpha) \sin(\eta) \cos(\alpha) \\ B &= \sin^2(\alpha) \sin(\theta_2) \\ C &= (\sin(\alpha) \cos(\eta) - \sin(\eta) \cos(\alpha) \cos(\theta_2)) \sin(\alpha) \end{aligned}$$

The components of f_3 and f_4 expressed in R_2 read as

$$\begin{aligned} [f_{3x} \ f_{3y} \ f_{3z} \ 1]^t &= Rot_z(\theta_2)Rot_x(\alpha)Rot_z(\theta_3) \\ &Rot_x\left(\frac{\eta}{2}\right)Rot_y(\theta_6) [1 \ 0 \ 0 \ 0]^t \end{aligned} \quad (14)$$

$$\begin{aligned} [f_{4x} \ f_{4y} \ f_{4z} \ 1]^t &= Rot_z(\theta_2)Rot_x(\alpha)Rot_z(\theta_3) \\ &Rot_x\left(\frac{\eta}{2}\right)Rot_y(\theta_6)Rot_y(\theta_7) [1 \ 0 \ 0 \ 0]^t \end{aligned} \quad (15)$$

Finally, the ratios $\frac{\Theta_2}{f_3}$ and $\frac{\Theta_2}{f_4}$ are calculated in R_1

$$\frac{\Theta_2}{f_3} = \frac{\dot{S}_{3x}}{\dot{\theta}_2} f_{3x} + \frac{\dot{S}_{3y}}{\dot{\theta}_2} f_{3y} + \frac{\dot{S}_{3z}}{\dot{\theta}_2} f_{3z} \quad (16)$$

$$\frac{\Theta_2}{f_4} = \frac{\dot{S}_{4x}}{\dot{\theta}_2} f_{4x} + \frac{\dot{S}_{4y}}{\dot{\theta}_2} f_{4y} + \frac{\dot{S}_{4z}}{\dot{\theta}_2} f_{4z} \quad (17)$$

whereas the ratios $\frac{\Theta_1}{f_3}$ and $\frac{\Theta_1}{f_4}$ read as (in R_1)

$$\frac{\Theta_1}{f_3} = (S_{3x}f_{3z} - S_{3z}f_{3x}) \quad \frac{\Theta_1}{f_4} = (S_{4x}f_{4z} - S_{4z}f_{4x}) \quad (18)$$

The ratios $\frac{\Theta_1}{f_1}$ and $\frac{\Theta_1}{f_2}$ are given by (with the positions S_1, S_2 given in the reference frame R_1)

$$\frac{\Theta_1}{f_1} = (S_{1x}f_{1z} - S_{1z}f_{1x}) \quad \frac{\Theta_1}{f_2} = (S_{2x}f_{2z} - S_{2z}f_{2x}) \quad (19)$$

with

$$\begin{aligned} f_{1x} &= \sin(m_1) \cos(\theta_2) + \sin(\theta_2) \cos\left(\frac{\alpha}{2}\right) \cos(m_1) \\ f_{1z} &= \left(\sin\left(\frac{\alpha}{2}\right) \cos\left(\frac{\eta}{2}\right) + \sin\left(\frac{\eta}{2}\right) \cos\left(\frac{\alpha}{2}\right) \cos(\theta_2) \right) \cos(m_1) \\ &\quad - \sin\left(\frac{\eta}{2}\right) \sin(m_1) \sin(\theta_2) \\ S_{1x} &= -k_1 \sin\left(\frac{\alpha}{2}\right) \sin(\theta_2) \\ S_{1z} &= k_1 \left(-\sin\left(\frac{\alpha}{2}\right) \sin\left(\frac{\eta}{2}\right) \cos(\theta_2) + \cos\left(\frac{\alpha}{2}\right) \cos\left(\frac{\eta}{2}\right) \right) \\ f_{2x} &= \sin(m_2) \cos(\theta_5) + \sin(\theta_5) \cos\left(\frac{\alpha}{2}\right) \cos(m_2) \\ f_{2z} &= \left(\sin\left(\frac{\alpha}{2}\right) \cos\left(\frac{\eta}{2}\right) - \sin\left(\frac{\eta}{2}\right) \cos\left(\frac{\alpha}{2}\right) \cos(\theta_5) \right) \cos(m_2) \\ &\quad + \sin\left(\frac{\eta}{2}\right) \sin(m_2) \sin(\theta_5) \\ S_{2x} &= -k_2 \sin\left(\frac{\alpha}{2}\right) \sin(\theta_5) \\ S_{2z} &= k_2 \left(\sin\left(\frac{\alpha}{2}\right) \sin\left(\frac{\eta}{2}\right) \cos(\theta_5) + \cos\left(\frac{\alpha}{2}\right) \cos\left(\frac{\eta}{2}\right) \right) \end{aligned}$$

with, if $0 < \theta_2$: $\theta_5 = -\text{atan}_2(B,A) - \text{acos}\left(\frac{C}{\sqrt{A^2+B^2}}\right)$

else :

$$\theta_5 = -\text{atan}_2(B,A) + \text{acos}\left(\frac{C}{\sqrt{A^2+B^2}}\right)$$

3.2 Matrix of torques ratios \mathbf{T}

The behaviour of the actuating mechanism is given by the matrix \mathbf{T} , which can be written as follows The actuation mechanism consists of four loops:

- A loop ($Loop_1$) with five revolute joints (O_2, O_3, P_6, V_1, P_1). As input, this loop has two degrees of freedom But only one if we consider the spherical mechanism. This DOF can be modelled according to θ_2 . The output of the mechanism can be modelled according to ψ_1, v_1, ψ_6 . V_1 is a virtual link introduced in section 3.2.1. We therefore calculate three torque ratios $\frac{\Gamma_1}{\Theta_2}, \frac{N_1}{\Theta_2}$ and $\frac{\Gamma_6}{\Theta_2}$.
- A loop ($Loop_2$) with four revolute joints (P_5, P_6, O_6, O_7) and two ball and socket joints (P_8, P_7). As input, this loop has three degrees of freedom mechanism that can be modelled according to $\theta_7, \psi_6, \theta_6$. The output of the mechanism can be modelled according to ψ_5 . We therefore calculate three torque ratios $\frac{\Gamma_5}{\Theta_7}, \frac{\Gamma_5}{\Gamma_6}$ and $\frac{\Gamma_5}{\Theta_6}$.
- A five-bar planar linkage ($Loop_3$) (P_2, P_3, P_4, P_5, V_1) which is connected to the spherical mechanism by two revolute joints P_1 and P_6 which are concurrent in the center of the spherical mechanism C and inscribed in the plane perpendicular to the links of the 5-bar planar mechanism. The joints (P_1, P_2) and (P_5, P_6) are equivalent to an universal joint. This loop has two degrees of freedom that can be modelled according to v_1, ψ_5 . The output of the mechanism can be modelled according to ψ_2 . We calculate two torque ratios $\frac{\Gamma_2}{N_1}$ and $\frac{\Gamma_2}{\Gamma_5}$.
- An actuated prismatic joint P_{10} connect by two ball and socket joint (P_9, P_{11}) and three revolute (O_1, P_1, P_2) ($Loop_4$). As input, this loop has three degrees of freedom mechanism that can be modelled according to θ_2, ψ_1, ψ_2 . The output of the mechanism is prismatic joint P_{10} . We therefore calculate three force ratios $\frac{F_{10}}{\Theta_1}, \frac{F_{10}}{\Gamma_1}$ and $\frac{F_{10}}{\Gamma_2}$.

3.2.1 Virtual 2-DOFs mechanism ($Loop_1$) A virtual mechanism with two degrees of freedom (v_1, ψ_1) is defined (P_1, V_1, P_6) to model the behaviour of the spherical mechanism on the first stage of the finger actuating mechanism (P_2, P_3, P_4, P_5). The link V_1 is defined as coincident at point C and perpendicular to the plane formed by the points P_1, C, P_6 . The virtual mechanism is connected to the point P_6 located on the spherical mechanism. Depending on the values of θ_2 , the spherical parallel mechanism admits two assembly modes, parallelogram mode and anti-parallelogram mode. The first mode is used in the finger movement and limits on the passive joints will be placed

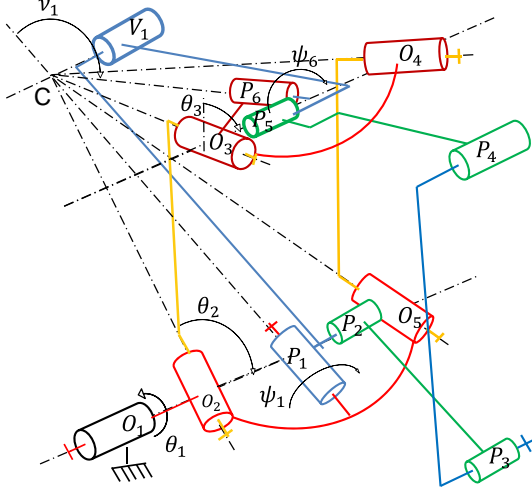


FIGURE 6: Virtual two-degree-of-freedom mechanism similar to the parallel-spherical mechanism

to avoid the singularity of the mechanism and the change of assembly mode. The direct kinematics of the virtual mechanism is defined as

$$v_1 = \text{acos} \left(\frac{-P_{6y} \sin(\frac{\eta}{2}) + P_{6x} \cos(\frac{\eta}{2})}{\cos(\frac{\eta}{2})} \right) \quad (20)$$

$$\text{If } P_{6y} > 0 \text{ then : } \psi_1 = -\text{acos} \left(-\frac{P_{6z}}{\sin(v_1) \cos(\frac{\eta}{2})} \right)$$

else :

$$\psi_1 = \text{acos} \left(-\frac{P_{6z}}{\sin(v_1) \cos(\frac{\eta}{2})} \right) \quad (21)$$

with $P_6 = [P_{6x}, P_{6y}, P_{6z}]^t$ defined as a function of the design parameters and the angles of the spherical parallel mechanism [9]:

$$P_{6x} = -\frac{(\cos(\eta) + 1) \cos(\alpha)}{2} + \frac{\sin(\alpha) \sin(\eta) \cos(\theta_3)}{2}$$

$$P_{6y} = \frac{((\cos^2(\eta) + 1) \sin(\alpha) + \sin(\eta) \cos(\alpha) \cos(\theta_3)) \cos(\theta_2)}{2} - \frac{\sin(\eta) \sin(\theta_2) \sin(\theta_3)}{2}$$

$$P_{6z} = -\frac{((\cos(\eta) + 1) \sin(\alpha) + \sin(\eta) \cos(\alpha) \cos(\theta_3)) \sin(\theta_2)}{2} - \frac{\sin(\eta) \sin(\theta_3) \cos(\theta_2)}{2}$$

Due to the symmetry of the spherical mechanism, we find

$$\psi_1 = -\psi_6. \quad (22)$$

The torque ratio $\frac{N_1}{\Theta_2}$ and $\frac{\Gamma_1}{\Theta_2}$ can be now written as

$$\frac{N_1}{\Theta_2} = -\text{asin} \left(\frac{\dot{P}_{6x} \cos(\frac{\eta}{2}) - \dot{P}_{6y} \sin(\frac{\eta}{2})}{\cos(\frac{\eta}{2})} \right) \quad (23)$$

if $P_{6y} > 0$:

$$\frac{\Gamma_1}{\Theta_2} = \frac{\Gamma_6}{\Theta_2} = -\frac{N_1 P_{6z} \cos(v_1) - \dot{P}_{6z} \sin(v_1)}{\sin^2(v_1) \cos(\frac{\eta}{2}) \sqrt{-\frac{P_{6z}^2}{\sin^2(v_1) \cos^2(\frac{\eta}{2})} + 1}} \quad (24)$$

else :

$$\frac{\Gamma_1}{\Theta_2} = \frac{\Gamma_6}{\Theta_2} = \frac{N_1 P_{6z} \cos(v_1) - \dot{P}_{6z} \sin(v_1)}{\sin^2(v_1) \cos(\frac{\eta}{2}) \sqrt{-\frac{P_{6z}^2}{\sin^2(v_1) \cos^2(\frac{\eta}{2})} + 1}} \quad (25)$$

based on the velocity of P_6 :

$$\frac{\dot{P}_{6x}}{\theta_2} = -z_1 ((-\dot{\theta}_3 \sin(\theta_2) \sin(\theta_3) \cos(\alpha) + \dot{\theta}_3 \cos(\theta_2) \cos(\theta_3)) - \sin(\theta_2) \sin(\theta_3) + \cos(\alpha) \cos(\theta_2) \cos(\theta_3)) \sin(\frac{\eta}{2}) + \sin(\alpha) \cos(\frac{\eta}{2}) \cos(\theta_2) \quad (26)$$

$$\frac{\dot{P}_{6y}}{\theta_2} = -z_1 ((\dot{\theta}_3 \sin(\theta_2) \cos(\theta_3) + \dot{\theta}_3 \sin(\theta_3) \cos(\alpha) \cos(\theta_2)) + \sin(\theta_2) \cos(\alpha) \cos(\theta_3) + \sin(\theta_3) \cos(\theta_2)) \sin(\frac{\eta}{2}) + \sin(\alpha) \sin(\theta_2) \cos(\frac{\eta}{2}) \quad (27)$$

$$\frac{\dot{P}_{6z}}{\theta_2} = -z_1 \dot{\theta}_3 \sin(\alpha) \sin(\frac{\eta}{2}) \sin(\theta_3) \quad (28)$$

3.2.2 Evaluation of Γ_5/Θ_7 (Loop2) The mechanism formed by the joints $(O_7, P_8, P_9, P_5, P_6, O_6)$ is a three degrees of freedom mechanism that can be modelled according to $\theta_7, \psi_6, \theta_6$. The angles θ_7, θ_6 are degrees of freedom corresponding to the movements of the intermediate and distal phalanges and the angle ψ_6 is related to the motions of the spherical parallel mechanism θ_2 by Eqs. (22) and (21). Θ_7 is the torque in the joint O_7 and Γ_5 is the torque in the link P_5 , to calculate the torque ratio $\frac{\Gamma_5}{\Theta_7}$, we define RSSR mechanism with one degree of freedom [13] with four joints (O_7, P_8, P_9, P_5) . The joints P_6 and O_6 are defined

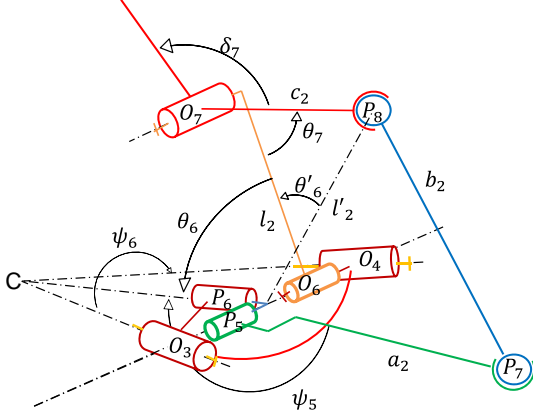


FIGURE 7: Mechanism *RSSR*

in the matrix M_{O75} of Eq. (29) of transfer between links (O_7, P_5) .

$$M_{O75} = \begin{bmatrix} s_{11} & s_{12} & s_{13} & X_{01} \\ s_{21} & s_{22} & s_{23} & Y_{01} \\ s_{31} & s_{32} & s_{33} & Z_{01} \\ 0 & 0 & 0 & 1 \end{bmatrix} \quad (29)$$

$$= \begin{bmatrix} -\cos(\theta_6) & -\sin(\theta_6)\cos(\psi_6) & \sin(\psi_6)\sin(\theta_6) & l_2 \\ \sin(\theta_6) & -\cos(\psi_6)\cos(\theta_6) & \sin(\psi_6)\cos(\theta_6) & 0 \\ 0 & \sin(\psi_6) & \cos(\psi_6) & 0 \\ 0 & 0 & 0 & 1 \end{bmatrix}$$

The torque ratio $\frac{\Gamma_5}{\Theta_7}$ can be now written as

$$\frac{\Gamma_5}{\Theta_7} = \frac{d' \cos(\psi_5) + e' \sin(\psi_5) - f'}{d \sin(\psi_5) - e \cos(\psi_5)} \quad (30)$$

with $d' = 2a_2c_2s_{11}\sin(\theta_7) - 2a_2c_2s_{21}\cos(\theta_7)$, $e' = 2a_2c_2s_{12}\sin(\theta_7) - 2a_2c_2s_{22}\cos(\theta_7)$, $f' = -2X_{01}c_2\sin(\theta_7)$, and where ψ_5 is the angle between $\overrightarrow{P_5C}$ and $\overrightarrow{P_5P_7}$ as defined as following

$$\psi_5 = \text{atan}_2(e, d) - \text{acos}\left(\frac{f}{\sqrt{d^2 + e^2}}\right) \quad (31)$$

with $d = -2a_2c_2s_{21}\sin(\theta_7) + 2a_2s_{11}(X_{01} - c_2\cos(\theta_7))$, $e = -2a_2c_2s_{22}\sin(\theta_7) + 2a_2s_{12}(X_{01} - c_2\cos(\theta_7))$ and $f = -X_{01}^2 + 2X_{01}c_2\cos(\theta_7) - a_2^2 + b_2^2 - c_2^2$.

3.2.3 Evaluation of Γ_5/Θ_6 (Loop₂) In a similar way, to calculate Γ_5 according to Θ_7 , we calculate torque ratio $\frac{\Gamma_5}{\Theta_6}$,

where Θ_6 is the torque in the joint O_6 . We define the *RSSR* mechanism with one degree of freedom [13] with for joints (O_6, P_8, P_9, P_5) . The joint P_6 is defined by the matrix M_{O65} Eq. (32) of transfer between links O_6, P_5 .

$$M_{O65} = \begin{bmatrix} 1 & 0 & 0 & 0 \\ 0 & \cos(\psi_6) & -\sin(\psi_6) & 0 \\ 0 & \sin(\psi_6) & \cos(\psi_6) & 0 \\ 0 & 0 & 0 & 1 \end{bmatrix} \quad (32)$$

We introduce two new variables θ'_6, l'_2 associated with the links (O_6, P_8) .

$$l'_2 = \sqrt{c_2^2 - 2c_2l_2\cos(\theta_7) + l_2^2} \quad (33)$$

if $\pi < \theta_7 < 2\pi$:

$$\theta'_6 = \text{acos}\left(\frac{l_2^2 + (l'_2)^2 - c_2^2}{2l_2l'_2}\right)$$

else :

$$\theta'_6 = -\text{acos}\left(\frac{l_2^2 + (l'_2)^2 - c_2^2}{2l_2l'_2}\right) \quad (34)$$

The torque ratio $\frac{\Gamma_5}{\Theta_6}$ can be now written as

$$\frac{\Gamma_5}{\Theta_6} = \frac{-d' \cos(\psi_5) - e' \sin(\psi_5)}{d \sin(\psi_5) - e \cos(\psi_5)} \quad (35)$$

with $d' = 2a_2l'_2\sin(\theta_6 + \theta'_6)$, $e' = -2a_2l'_2\cos(\psi_6)\cos(\theta_6 + \theta'_6)$, $d = -2a_2l'_2\cos(\theta_6 + \theta'_6)$ and $e = -2a_2l'_2\cos(\psi_6)\sin(\theta_6 + \theta'_6)$.

3.2.4 Evaluation of Γ_5/Γ_6 (Loop₂) In a similar way, to calculate Γ_5 according to Θ_7 , we calculate $\frac{\Gamma_5}{\Gamma_6}$, where Γ_6 is the torque in the joint P_6 Eq. (25). We define the *RSSR* mechanism with one degree of freedom [13] with for joints (P_6, P_8, P_9, P_5) . The the matrix M_{P65} Eq. (36) is matrix of transfer between links P_6, P_5 .

$$M_{P65} = \begin{bmatrix} 0 & -1 & 0 & 0 \\ 0 & 0 & -1 & 0 \\ 1 & 0 & 0 & Z_{P6P8} \\ 0 & 0 & 0 & 1 \end{bmatrix} \quad (36)$$

We introduce two new variables Z_{P6P8}, l''_2 associated with the links (P_6, P_8) .

$$l''_2 = c_2 \sin(\theta_6 + \theta_7) - l_2 \sin(\theta_6) \quad (37)$$

$$Z_{P6P8} = c_2 \sin(\theta_6 + \theta_7) - l_2 \sin(\theta_6) \quad (38)$$

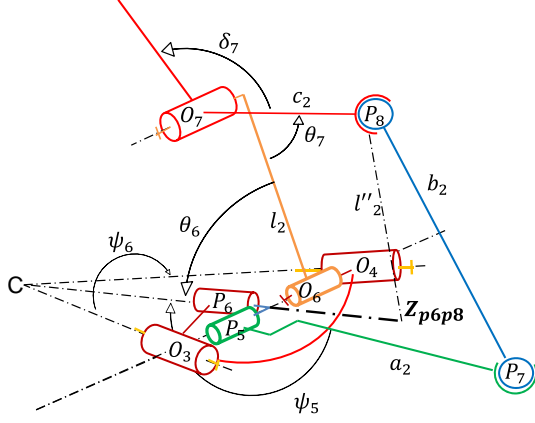


FIGURE 8: Mechanism $RSSR \Gamma_5(\Gamma_6)$

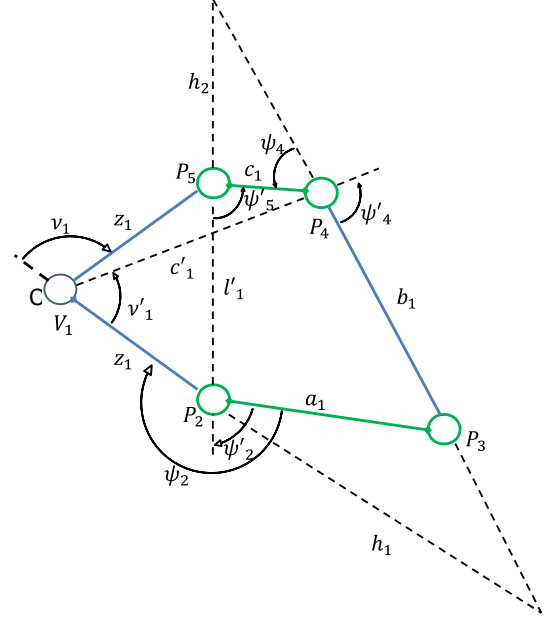


FIGURE 9: Actuation coupling mechanism

The torque ratio $\frac{\Gamma_5}{\Gamma_6}$ can be now written as

$$\frac{\Gamma_5}{\Gamma_6} = \frac{de'}{d^2 + e^2} - \frac{d'e'f}{(d^2 + e^2)\sqrt{d^2 + e^2 - f^2}} \quad (39)$$

with $d' = 2a_2l_2'' \cos(\psi_6)$, $e' = -2a_2l_2'' \sin(\psi_6)$, $d = 2Z_{P_6P_8}a_2$, $e = 2a_2l_2'' \cos(\psi_6)$ and $f = -Z_{P_6P_8}^2 - a_2^2 + b_2^2 - (l_2'')^2$.

3.2.5 Evaluation of Γ_2/Γ_5 and Γ_2/N_1 (Loop₃) The joints (P_5, P_4, P_3, P_2, V_1) form a closed loop with two degrees of freedom (Figure 9). v_1 is linked to the movements of the spherical mechanism θ_2 by Eq. (20) and ψ_5 is calculated in Eq. (31). To calculate the torque ratio $\frac{\Gamma_2}{\Gamma_5}$, we define the 4R mechanism [9] plane with for the articulations (P_5, P_4, P_3, P_2).

To do this, we define three new variables: l'_1 distance between P_5, P_2 , ψ'_5 the angle between $\vec{P_5P_7}$ and $\vec{P_5P_2}$ and z_1 distance between CP_1 and CP_5

$$z_1 = \frac{l_1 \cos\left(\frac{\eta}{2}\right)}{2 \sin\left(\frac{\alpha}{2}\right)} \quad (40)$$

We deduce from this

$$l'_1 = 2z_1 \cos\left(\frac{v_1}{2}\right) \quad (41)$$

with v_1 defined in Eq. (20)

$$\psi'_5 = -\frac{v_1}{2} - \psi_5 \quad (42)$$

The angles ψ_4 are written as a function of ψ'_5

$$\psi_4(\psi'_5) = \text{atan}_2(B, A) - \text{acos}\left(\frac{C}{\sqrt{A^2 + B^2}}\right) \quad (43)$$

with $A(\psi'_5) = 2b_1c_1 - 2b_1l'_1 \cos(\psi'_5)$, $B(\psi'_5) = 2b_1l'_1 \sin(\psi'_5)$ and $C(\psi'_5) = a_1^2 - b_1^2 - c_1^2 + 2c_1l'_1 \cos(\psi'_5) - (l'_1)^2$.

The torque ratio $\frac{\Gamma_2}{\Gamma_5}$ can be now written as

$$\frac{\Gamma_2}{\Gamma_5} = \frac{h_2}{h_2 + l'_1} \quad (44)$$

$$\text{with } h_2 = -\frac{c_1 \sin(\psi_4)}{\sin(\psi_4 + \psi'_5)}$$

To calculate the torque ratio $\frac{\Gamma_2}{N_1}$, we define the 4R mechanism [9] plane with for the articulations (V_1, P_4, P_3, P_2). To do this, we define three new variables: c'_1 distance between V_1, P_4 , v'_1 the angle between $\vec{V_1P_4}$ and $\vec{V_1P_2}$ and ψ'_4 the angle between $\vec{P_4V_1}$ and $\vec{P_4P_3}$

$$c'_1 = \sqrt{c_1^2 - 2c_1z_1 \cos(\psi_6) + z_1^2} \quad (45)$$

$$v'_1 = -v_1 - \text{acos}\left(\frac{-c_1^2 + (c'_1)^2 + z_1^2}{2c'_1z_1}\right) + \pi \quad (46)$$

The angle ψ'_4 as a function of v'_1 is defined

$$\psi'_4(v'_1) = \text{atan}_2(B, A) - \text{acos}\left(\frac{C}{\sqrt{A^2 + B^2}}\right) \quad (47)$$

with $A(v'_1) = 2b_1c'_1 - 2b_1z_1 \cos(v'_1)$, $B(v'_1) = 2b_1z_1 \sin(v'_1)$ and $C(v'_1) = a_1^2 - b_1^2 - (c'_1)^2 + 2c'_1z_1 \cos(v'_1) - z_1^2$.

$$h_1 = -\frac{c'_1 \sin(\psi'_4)}{\sin(v'_1 + \psi'_4)} \quad (48)$$

The torque ratio $\frac{\Gamma_2}{N_1}$ can be now written as

$$\frac{\Gamma_2}{N_1} = -\frac{h_1}{h_1 + z_1} \quad (49)$$

The angles ψ_2 and ψ'_2 are calculated to allow the calculation of the force on the actuator.

$$\psi_2(\psi'_5) = \psi'_2(\psi'_5) - \frac{v_1}{2} \quad (50)$$

$$\psi'_2(\psi'_5) = \text{atan}\left(\frac{B}{A}\right) - \text{acos}\left(\frac{C}{\sqrt{A^2 + B^2}}\right) \quad (51)$$

with $A(\psi'_5) = 2a_1c_1 \cos(\psi'_5) - 2a_1l_1$, $B(\psi'_5) = 2a_1c_1 \sin(\psi'_5)$ and $C(\psi'_5) = a_1^2 - b_1^2 + c_1^2 - 2c_1l_1 \cos(\psi'_5) + l_1^2$.

3.2.6 Actuating loop (Loop₄) Finger actuation is done with the prismatic link P_{10} which is connected to two ball-and-socket joints P_9 and P_{11} . The distance between P_9 and P_{11} is named d_0 , where a_0 and c_0 are the lengths between P_9 and O_1 , P_{11} and O_1 , respectively.

$$d_0 = \sqrt{a_0^2 + 2a_0c_0(\sin(\psi_2)\sin(\theta_1)\cos(\psi_1) + \cos(\psi_2)\cos(\theta_1)) + c_0^2}$$

We derive d_0 according to ψ_2 , ψ_1 and θ_1 to obtain $\frac{F_{10}}{\Gamma_2}$, $\frac{F_{10}}{\Gamma_1}$, $\frac{F_{10}}{\Theta_1}$ where F_{10} is the force produced by the actuator.

$$\begin{aligned} \frac{F_{10}}{\Gamma_2} &= \frac{a_0c_0(\sin(\psi_2)\cos(\theta_1) - \sin(\theta_1)\cos(\psi_1)\cos(\psi_2))}{d_0} \\ \frac{F_{10}}{\Gamma_1} &= -\frac{a_0c_0\sin(\psi_1)\sin(\psi_2)\sin(\theta_1)}{d_0} \\ \frac{F_{10}}{\Theta_1} &= \frac{a_0c_0(\sin(\psi_2)\cos(\psi_1)\cos(\theta_1) - \sin(\theta_1)\cos(\psi_2))}{d_0} \end{aligned}$$

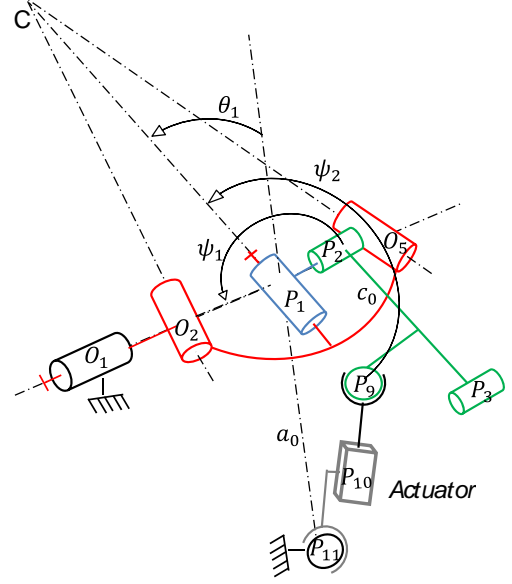


FIGURE 10: Actuating loop (Loop₄)

3.2.7 Evaluation of matrix \mathbf{T} From the previous results, it is now possible to write the matrix \mathbf{T} as follows

$$\mathbf{T} = \begin{bmatrix} -\frac{F_{10}}{\Theta_1} & -\frac{F_{10}}{\Theta_2} & -\frac{\Gamma_2}{\Theta_6} \frac{\Gamma_2}{\Gamma_5} \frac{F_{10}}{\Gamma_2} & -\frac{\Gamma_5}{\Theta_7} \frac{\Gamma_2}{\Gamma_5} \frac{F_{10}}{\Gamma_2} \\ 0 & 1 & 0 & 0 \\ 0 & 0 & 1 & 0 \\ 0 & 0 & 0 & 1 \end{bmatrix} \quad (52)$$

where $\frac{F_{10}}{\Theta_2} = \left(\frac{\Gamma_1}{\Theta_2} \frac{F_{10}}{\Gamma_1} + \frac{N_1}{\Theta_2} \frac{\Gamma_2}{N_1} \frac{F_{10}}{\Gamma_2} + \frac{\Gamma_6}{\Theta_2} \frac{\Gamma_5}{\Gamma_6} \frac{\Gamma_2}{\Gamma_5} \frac{F_{10}}{\Gamma_2} \right)$ consists of three terms because when the parallel spherical mechanism moves, it influences all the loops of the mechanism.

3.3 Input-output analysis for stability analysis

The input force $\mathbf{t} = [f_{10} \ 0 \ 0 \ 0]^t$ is defined by the action forces with the return springs are neglected and the output forces $\mathbf{f} = [f_1 \ f_2 \ f_3 \ f_4]^t$ are defined by the contact forces applied by the finger to the object. Stable configurations can be found in Fig. 11 with Tab. 1. The movement θ_2 causes limited variation in strength f_1 where θ_1 , θ_7 (See Eq. (4)) and m_1 , m_2 (See Eq. (6)) are in home position.

4 Conclusions

The main contribution of this article is a new kinematics allowing complex grasps with a spatial under-actuated mechanism. A spherical parallel mechanism has been added to the classical under-actuated fingers in order to adjust the fingers from a neutral position to a spherical or cylindrical grasp. The stability of

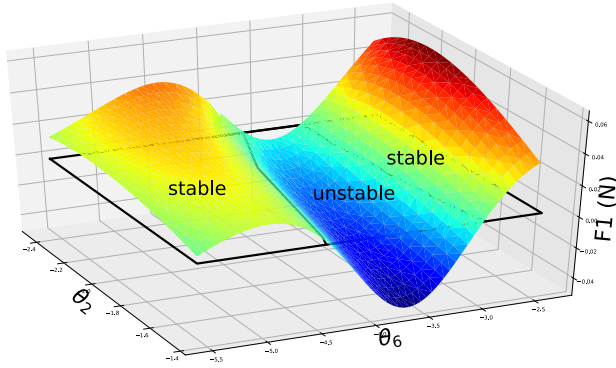


FIGURE 11: Stability condition for f_1 (N) versus θ_2 and θ_6 [rad].

TABLE 1: Design parameters

l_1	l_2	l_3	a_0	a_{123}	b_i	c_0	c_{123}
61	41	38	100	38	58	28	16
k_{12}	k_3	k_4	q_i	δ_7	α	η	f_{10}
$l_1/2$	$l_2/2$	$l_3/2$	0	$\pi/2$	85deg	40deg	1 N

this new robotic hand was analysed using two Jacobian matrices. Compared to the modelling of planar under-actuated fingers, new components have been added to the Jacobian matrix. The contact surfaces are simplified by point contacts. In this article, the interaction between the different fingers to allow a stable grip is not studied and will be the subject of further work. Future work will also be carried out to optimize the design parameters of the fingers for a family of parts from industry.

Acknowledgements

This work comes from a PhD thesis granted by ANRT (CIFRE program).

REFERENCES

- [1] Okada, T., 1982. “Computer control of multijointed finger system for precise object-handling”. *IEEE Transactions on Systems, Man, and Cybernetics*, **12**(3), pp. 289–299.
- [2] Salisbury, J. K., and Craig, J. J., 1982. “Articulated hands: Force control and kinematic issues”. *The International journal of Robotics research*, **1**(1), pp. 4–17.
- [3] Jacobsen, S., Iversen, E., Knutti, D., Johnson, R., and Biggers, K., 1986. “Design of the utah/mit dextrous hand”. In Proceedings. 1986 IEEE International Conference on Robotics and Automation, Vol. 3, IEEE, pp. 1520–1532.
- [4] Gazeau, J.-P., Zehloul, S., Arsicault, M., and Lallemand, J.-P., 2001. “The lms hand: force and position controls in the aim of the fine manipulation of objects”. In Proceedings 2001 ICRA. IEEE International Conference on Robotics and Automation, Vol. 3, Ieee, pp. 2642–2648.
- [5] Akin, D. L., Carignan, C. R., and Foster, A. W., 2002. “Development of a four-fingered dextrous robot end effector for space operations”. In Proceedings 2002 IEEE International Conference on Robotics and Automation, Vol. 3, IEEE, pp. 2302–2308.
- [6] Crisman, J. D., Kanojia, C., and Zeid, I., 1996. “Graspar: A flexible, easily controllable robotic hand”. *IEEE Robotics & Automation Magazine*, **3**(2), pp. 32–38.
- [7] Laliberté, T., and Gosselin, C. M., 1998. “Simulation and design of underactuated mechanical hands”. *Mechanism and machine theory*, **33**(1-2), pp. 39–57.
- [8] Cutkosky, M. R., et al., 1989. “On grasp choice, grasp models, and the design of hands for manufacturing tasks”. *IEEE Transactions on robotics and automation*, **5**(3), pp. 269–279.
- [9] McCarthy, J. M., and Soh, G. S., 2010. *Geometric design of linkages*, Vol. 11. Springer Science & Business Media.
- [10] Todhunter, I., 1863. *Spherical trigonometry, for the use of colleges and schools: with numerous examples*. Macmillan.
- [11] Birglen, L., Laliberté, T., and Gosselin, C. M., 2007. *Underactuated robotic hands*, Vol. 40. Springer.
- [12] Birglen, L., and Gosselin, C. M., 2004. “Kinetostatic analysis of underactuated fingers”. *IEEE Transactions on Robotics and Automation*, **20**(2), pp. 211–221.
- [13] Mazzotti, C., Troncossi, M., and Parenti-Castelli, V., 2017. “Dimensional synthesis of the optimal rrrr mechanism for a set of variable design parameters”. *Meccanica*, **52**(10), pp. 2439–2447.